Separation Science and Technology
Publication details, including instructions for authors and subscription information:
http://www.informaworld.com/smpp/title~content=t713708471

Separation of ibuprofen enantiomers by supercritical fluid simulated moving bed chromatography

S. Peper[a]; M. Lübbert[a]; M. Johannsen[a]; G. Brunner[a]
[a] Technical University Hamburg-Harburg, Hamburg, Germany

Online publication date: 07 October 2002

To cite this Article Peper, S. , Lübbert, M. , Johannsen, M. and Brunner, G.(2002) 'Separation of ibuprofen enantiomers by supercritical fluid simulated moving bed chromatography', Separation Science and Technology, 37: 11, 2545 — 2566
To link to this Article: DOI: 10.1081/SS-120004452
URL: http://dx.doi.org/10.1081/SS-120004452

SEPARATION SCIENCE AND TECHNOLOGY, 37(11), 2545–2566 (2002)

SEPARATION OF IBUPROFEN ENANTIOMERS BY SUPERCRITICAL FLUID SIMULATED MOVING BED CHROMATOGRAPHY

S. Peper,* M. Lübbert, M. Johannsen, and G. Brunner

Thermal Separation Processes, Technical University Hamburg-Harburg, Hamburg, Germany

ABSTRACT

The continuous separation of *R*(−)-ibuprofen and *S*(+)-ibuprofen by supercritical fluid simulated moving bed chromatography has been developed. First, experiments were performed at a low concentration level. Therefore, a starting set of operating parameters was calculated using the "triangle theory," which has been developed in the frame of equilibrium theory. Subsequently, the feed concentration was increased. A dynamic simulation program, based on a plug flow model with axial dispersion and linear mass transfer resistance, was used to predict the effect of operating variables on the process performance. Adsorption isotherms were determined with the elution by a characteristic point method. The experimental results were compared both with the model predictions based on the triangle theory and with the results of simulations.

*Corresponding author. Fax: 0049-40-42878-4072; E-mail: s.peper@tu-harburg.de

INTRODUCTION

Simulated moving bed (SMB) chromatography is a powerful purification process allowing the continuous separation of a feed mixture into two streams of products. The conventional co-current elution chromatography is discontinuous; the products are diluted and the productivity is low, which means that only a small amount of the product is separated per amount of stationary phase and time. To overcome these drawbacks, the SMB concept was developed. It is a counter-current process with reduced solvent consumption and high separating power (1). The counter-current flow is simulated by periodically switching the ports of the inlet (feed, desorbent) and the outlet (raffinate, extract, recycling) lines in the same direction as the fluid flow. In Fig. 1, the scheme of a SMB process is shown. A more detailed description of the SMB process is given for example in Ref. (2).

The SMB technique was originally developed in the 1960s by United Oil Products (UOP) (3) for the separation of hydrocarbons. In the last decade, this technique has been applied for a number of other separations such as sugars (4,5), racemic drugs (6–9), isomers (10), and enzymes (11,12). All these studies have been carried out using liquid solvents.

To date, only a few experimental results of SMB separation using supercritical carbon dioxide as mobile phase have been published (13–15). The combination of SMB technique with supercritical fluid chromatography (SFC)

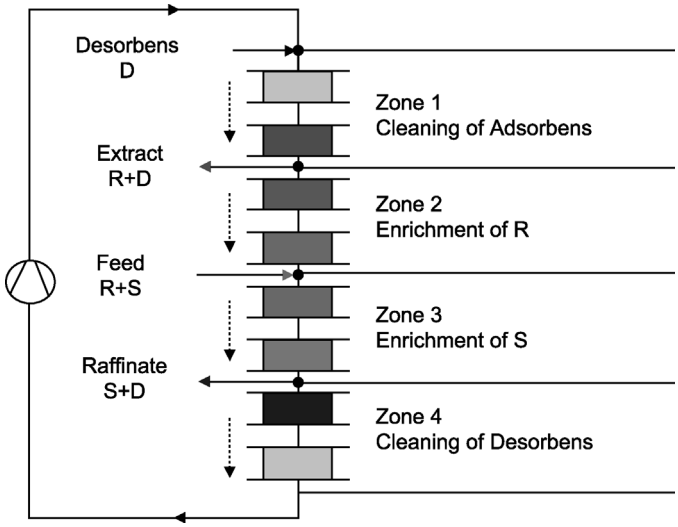

Figure 1. Scheme of the SMB process. *R*: more-retained compound; *S*: less-retained compound.

leads to an apparatus with unique features. Besides the above-mentioned advantages of the SMB process, the use of supercritical carbon dioxide as mobile phase offers an easy eluent–solute separation and eluent recycle, a low pressure drop, and high efficiency. Another unique feature of using supercritical fluids is the opportunity to change the elution strength of the mobile phase by density in order to optimize the separation performance (16).

The development of a method for an SFC-based separation of the ibuprofen enantiomers in analytical scale was published by Johannsen (17). Different chiral stationary phases were tested in analytical scale. Among the tested stationary phases, Kromasil CHI-TBB is the best-suited stationary phase for the separation of ibuprofen (17). The aim of this work is to show the feasibility of a SFC-SMB separation of *R*(−)- and *S*(+)-ibuprofen. Low concentration separations should be compared with model predictions based on equilibrium theory. The productivity of the process should be increased with the help of a simulation program. A simple design criteria exists for the separation of mixtures in the linear part of adsorption isotherms (18), but it is well known that they are of little use if nonlinear effects are taken into consideration. In the first step, SFC-SMB runs have been carried out with diluted feed. In that case, the adsorption equilibrium can be described by a linear adsorption isotherm. A starting set of operating parameters was calculated with the information available from typical elution chromatograms and the constructive parameters of the SMB apparatus. The model predictions closely agree with the experimental results. Purities higher than 98% were obtained. For further optimization, the knowledge of adsorption isotherms is absolutely necessary. After determining the adsorption isotherms with the elution by a characteristic point (ECP) method, the process was optimized with the help of a simulation program.

PROCEDURE FOR DETERMINING THE OPERATING CONDITIONS

To achieve complete separation of two components, proper operating conditions of the SMB unit must be selected. Storti et al. (18) have described a method for determining operating conditions based on the equilibrium theory (i.e., neglecting axial dispersion and mass transfer resistance). With this method, sometimes called "triangle theory," the true moving bed (TMB) process as well as the SMB process can be described with four key parameters: the net flow ratios m_j, one for each zone defined as ($j = 1, \ldots, 4$) :

$$m_j = \frac{\dot{V}_j^{\mathrm{SMB}} t_{\mathrm{shift}} - V\varepsilon}{V(1-\varepsilon)} \tag{1}$$

To achieve separation of the feed components, the net flow rates of the four zones of the SMB process must be set in such a way that the more-retained component will be transported to the extract port, while the less-retained component will be transported to the raffinate port. The actual separation of the components takes place in zones 2 and 3. It is rather useful to consider the projection of the regions of separation onto a (m_2, m_3) plane where the different separation regions are drawn in terms of purity of the outlet streams. In linear chromatography, the boundaries of the region of complete separation are given by the linear adsorption parameters H_i. The linear adsorption parameter is related to the retention time in a chromatographic column $t_{R,i}$ by the following equation:

$$t_{R,i} = t_0\left(1 + \frac{1-\varepsilon}{\varepsilon}H_i\right) \tag{2}$$

Using the net flow ratios, the conditions for complete separation are given by the following constraints for the case $H_{A,i} > H_{B,i}$ (18,19):

$$\begin{aligned} &H_{A,1} < m_1 \\ &H_{B,2} < m_2 < H_{A,2} \\ &H_{B,3} < m_3 < H_{A,3} \\ &m_4 < H_{B,4} \end{aligned} \tag{3}$$

A positive feed flow rate requires $m_3 > m_2$, hence the second and third inequality of Eq. (3) can be recast in the following form: $H_B < m_2 < m_3 < H_A$. If the process is operated in the pressure gradient mode, the pressure and density of the mobile phase are different in each zone of the unit. Therefore, the linear adsorption parameter of the same solute changes from one zone to the following one. If it is assumed that the elution strength of the mobile phase decreases with decreasing pressure/density, the retention of the two solutes should also decrease along the SMB unit operated in the pressure gradient mode. As a consequence of this, it is observed that

$$H_{i,1} < H_{i,2} < H_{i,3} < H_{i,4}. \tag{4}$$

Accordingly, with a decreasing pressure gradient from zone 1 to zone 4, a decreasing gradient of the elution strength of the mobile phase is realized. In case of a maximum elution strength in the first zone, where the more-retained component must be eluted, and a minimum elution strength in the fourth zone, where the less-retained component must be retained by the stationary phase, together with a similar positive effect on the performances of zone 2 and 3, the

separation performance related to productivity and mobile phase consumption can be optimized.

By applying the inequalities of Eq. (3), the region of complete separation can be projected onto the (m_2, m_3) plane similar to the isocratic case. In Fig. 2, the regions of the (m_2, m_3) plane are shown for the pressure gradient mode with $H_{A,2} > H_{B,3}$.

It was shown that the specific solvent consumption and specific productivity per unit mass of stationary phase improves while moving away from the diagonal in the (m_2, m_3) plane, and reaches the optimal values on the vertex of the complete separation region (19). Further details of the triangle theory can be found in literature (19–21).

As mentioned before, it is relatively easy to determine the exact coordinates of the complete separation region in a (m_2, m_3) plane in linear chromatography. However, this (m_2, m_3) plane has a low significance for the separation of mixtures characterized by nonlinear adsorption equilibrium. In that case, the shape and location of the complete separation region change and can be calculated analytically only in special cases (e.g., Langmuir isotherm (22)). Furthermore, these analytical solutions are based on the equilibrium theory, and therefore, neglect the mass transfer resistance and axial dispersion. In addition, the number of columns used in the SMB process is not taken into account by the analytical solution because it is based on the

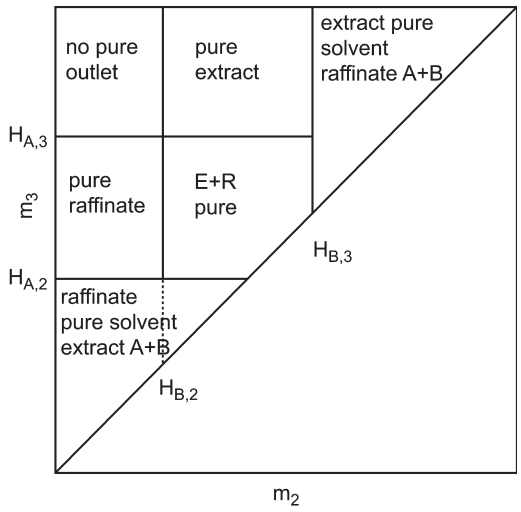

Figure 2. Regions of the (m_2, m_3) plane with different separation regimes in terms of purity of the outlet streams for a system described by the linear adsorption isotherm.

TMB process. For that reason, a more detailed simulation program was used for the investigation of increasing productivity. The program used simulates the SFC-SMB process dynamically, which implies that the switching of the valves are explicitly mentioned. For the dynamic simulation, a plug flow model with axial dispersion and linear mass transfer resistance was used. The solution of the resulting mass balance equations was performed with a finite difference method, first developed by Rouchon et al. (23) and adapted to the conditions of the SMB process by Kniep et al. (24). The pressure drop in the columns was calculated with the Darcy equation. The equation of state from Span and Wagner (25) was used to calculate the mobile phase density. The density of the mobile phase was considered as variable.

Due to the fact that the pressure drop in the columns leads to a variable volume flow in the different zones of the SMB, a new parameter m_j^* (constant for each zone), based on the mass flows in the different SMB zones, were defined (26):

$$m_j^* = \frac{\dot{V}_j^{\mathrm{SMB}} t_{\mathrm{shift}} \rho_{\mathrm{mobile\ phase}} - V\varepsilon\rho_{\mathrm{ref}}}{V(1-\varepsilon)\rho_{\mathrm{ref}}} \tag{5}$$

The algorithm mentioned is fast and robust enough to calculate the region of complete separation in the (m_2^*, m_3^*) plane numerically considering the effects of axial dispersion and a discrete number of columns in an SMB process.

EXPERIMENTAL

Materials

Carbon dioxide for adsorption measurements and preparative separation was obtained from KWD (Bad Hönningen, Germany) with a purity of more than 99.95%. Isopropanol (IPA; >99.95%) used as a modifier and *n*-hexane (>99.99%) were purchased from Merck (Darmstadt, Germany). 1,3,5 tri-*tert*-butyl-benzene (≥97%) and *S*(+)-ibuprofen (≥99%) were purchased from Fluka (Deisenhofen, Germany). Ibuprofen racemate (99.3%) was kindly donated by Omya Peralta (Hamburg, Germany). The analytical and preparative columns were packed with Kromasil CHI-TBB, 10 μm, kindly donated by Eka Chemicals, Bohus, Sweden.

The SFC-SMB

The SFC-SMB plant (Fig. 3) consists of eight custom-made columns (inner diameter 30 mm) with dynamic axial compression and variable bed length. The

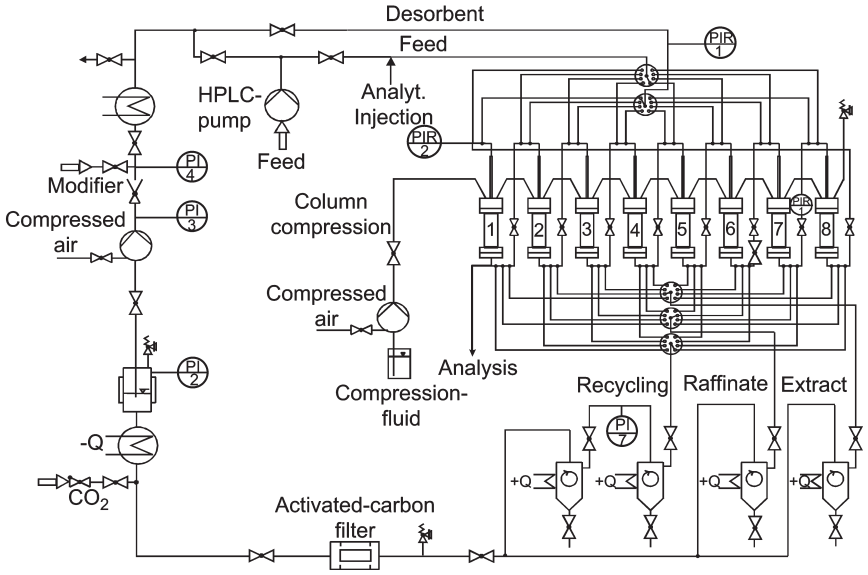

Figure 3. Scheme of the SFC-SMB plant.

columns are designed for pressures up to 40 MPa and temperatures up to 200°C. The five in- and out-going streams (feed, desorbents, raffinate, extract, and recycling) are guided by five 8 + 1 way valves. Between two columns, shut-off valves are located. All these valves are operated with air actuators. The raffinate and extract fractions were collected in high-pressure fluid cyclones, respectively. Both, columns and cyclones are electrically heated with heating tapes. Temperatures are measured with PT 100 resistors. From the bottom of an autoclave, liquid CO_2 is charged by an air-driven pump into the system up to flow rates of 18 kg/hr. Then, the carbon dioxide passes through a pressure-regulating valve, which regulates the pressure as desired. The modifier is added by a high-performance liquid chromatography (HPLC) pump. Heating is carried out in a temperature-controlled water bath. The stream is divided into two lines: one for the desorbents and one for the feed. The liquid feed material is charged into the system by a second HPLC pump. The mass flows of the feed-, extract-, raffinate-, and recycling-stream are measured by Rheonik mass flow detectors. A 100-μL sample loop is located between the columns 1 and 2 for the determination of the internal concentration profile. A more detailed description of the plant is published elsewhere (15).

Apparatus for Adsorption Measurements

Carbon dioxide is liquefied and compressed up to 40 MPa by a pneumatically driven pump. This process is carried out by a modified PM-101 module (NWA, Lörrach, Germany). Afterwards, the pressure is reduced to operating conditions by two pressure-reducing valves. With a syringe pump (260D, Isco, Lincoln NE), isopropanol is added to the carbon dioxide. Operating temperature is achieved with a heating cabinet (Binder, Tuttlingen, Germany) containing a 4.6×250 mm analytical column and a Rheodyne 6-port valve with a sample loop for injection. After detection with a UV detector (LCD 503, Gamma Anlagen Technik, Bremen, Germany), pressure is reduced to ambient conditions using a backpressure-controlled pressure-reducing valve. Carbon dioxide flow is measured with a gas meter (T63, Ritter, Bochum, Germany) at ambient pressure.

Determination of Adsorption Isotherms and Column Porosity

In preparative chromatography, the porosity of the stationary phase is an important parameter. It can be calculated from the retention volume of an unretained substance, the so-called hold-up volume. Different marker substances (1,3,5 tri-*tert*-butyl-benzene, *n*-hexane, and isopropanol) were used in order to quantify the hold-up volume of the Kromasil CHI-TBB column. As shown in Fig. 4, hexane is the most suitable substance for determining the porosity compared to 1,3,5 tri-*tert*-butyl-benzene and isopropanol. It shows the lowest holdup volume and no dependency between holdup volume and density of the mobile phase.

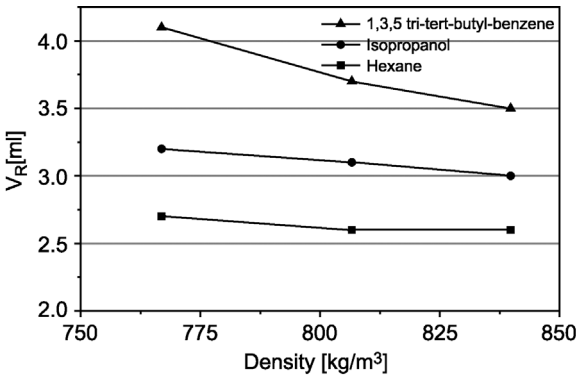

Figure 4. Retention volume of Kromasil CHI-TBB (analytical column) measured with different marker substances in subject to the density. $T = 40°C$, 4.5 wt.% IPA.

Adsorption isotherms were determined at a temperature of 40°C and pressures of 15.6 and 17 MPa. As there was only a limited amount of ibuprofen available and most of the substance were needed for process development, only peak experiments with ibuprofen dissolved in *n*-hexane were performed. Other experimental methods as such as breakthrough and perturbation analysis would have consumed large amounts of substance. From the shape of the analytical peaks, the Peclet number was estimated as 10,000. Due to this large number of theoretical plates, the ECP method was used for obtaining parameters. The porosity of the stationary phase was calculated from chromatograms of pure *n*-hexane.

As the isotherm was fitted to the peak shapes, a calibration between the detector output and concentration had to be performed. This was done by fitting the parameters of a polynomial so that the relation between peak area and injected mass was satisfied (Eq. (6)). This step was carried out for each enantiomer and pressure, respectively.

$$c_{\text{inj}} V_{\text{inj}} = \dot{V} \int c(t)\mathrm{d}t = \dot{V} \int [a_1 D(t) + a_2 D^2(t) + a_3 D^3(t)]\mathrm{d}t \tag{6}$$

The single-component adsorption is described using the Hill-isotherm (26). This model is obtained from statistical thermodynamics and can be fitted to a wide range of adsorption equilibria.

$$q = \frac{q_s}{n} \frac{b_1 c + 2b_2 c^2 + \cdots + n b_n c^n}{1 + b_1 c + b_2 c^2 + \cdots + b_n c^n} \tag{7}$$

For $n = 1$, the isotherm is identical to the Langmuir isotherm. For $n \geq 2$, it is possible to describe inflection points.

Parameter sets for various values of n were obtained by fitting the derivative of the isotherm to the tail of large peaks. In Fig. 5, deviations for $n = 1$ (Langmuir isotherm), $n = 2$ (quadratic isotherm), and $n = 3$ (cubic isotherm) are shown for the *S*-enantiomer at 17 MPa. As the cubic isotherm gives significantly better results for both enantiomers at both pressures, it is chosen for further description.

For describing binary adsorption, an ideal adsorbed solution (IAS) was assumed as described by Seidel and Gelbin (27). This theory allows the prediction of multi-component adsorption equilibria from single-component isotherms and does not require special mixture parameters.

In Table 1 and Fig. 6, the isotherms and their parameters are shown. It can be seen that the pressure dependency is very low. The maximum loading q_s is almost the same for both enantiomers at both pressures, respectively. These values refer to the overall particle volume. However, it has to be annotated that these values are obtained from lower concentrations, and therefore only represent an estimation.

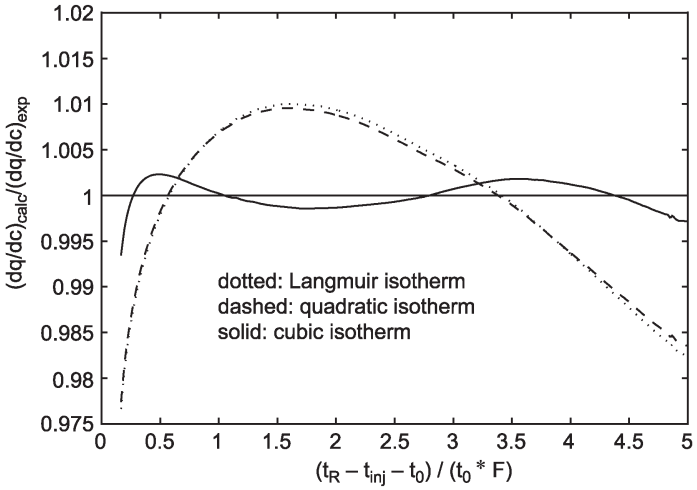

Figure 5. Deviations of isotherm models (*S*-enantiomer, 17 MPa).

The measured overall porosity of the analytical column is $\varepsilon = 0.703$. Isotherm parameters and Peclet number were checked by comparing the measured and simulated single component and mixture chromatograms.

In Figs. 7 and 8, experiments and simulations of both enantiomers and a racemic mixture are shown. In Fig. 7, an impurity of *S*-enantiomer elutes before the *R*-enantiomer. All simulations show a good agreement with the experiments.

Column Packing and Testing

The columns were packed by a slurry method: 50 g of stationary phase (Kromasil CHI-TBB) was slurried in 200 mL IPA and filled into the column. The

Table 1. Isotherm Parameters

$q = \frac{q_s}{3}\frac{b_1 c + 2b_2 c^2 + 3b_3 c^3}{1 + b_1 c + b_2 c^2 + b_3 c^3}$	q_s (kg/m^3)	b_1 (kg/m^3)$^{-1}$	b_2 (kg/m^3)$^{-2}$	b_3 (kg/m^3)$^{-3}$
S-Enantiomer (17 MPa)	146.1	0.1672	9.422×10^{-3}	6.133×10^{-4}
R-Enantiomer (17 MPa)	136.7	0.2136	1.564×10^{-2}	1.616×10^{-3}
S-Enantiomer (15.6 MPa)	125.0	0.1956	1.424×10^{-2}	1.088×10^{-3}
R-Enantiomer (15.6 Mpa)	126.6	0.2384	2.091×10^{-2}	1.725×10^{-3}

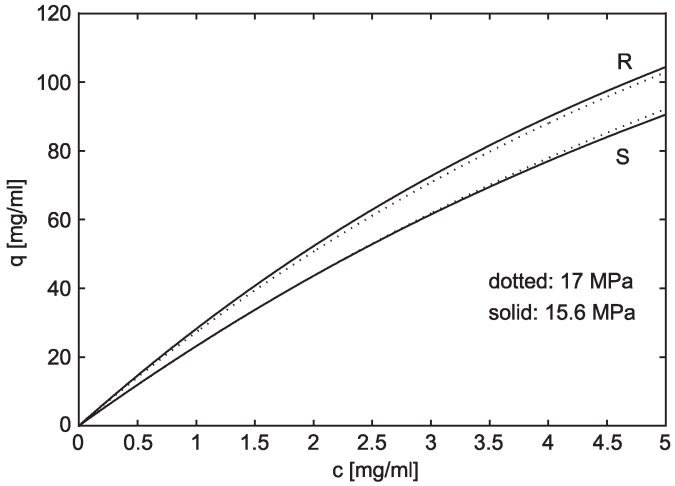

Figure 6. Ibuprofen isotherms for both enantiomers at 15.6 and 17 MPa.

IPA was discharged from the column using a vacuum pump. After mounting the columns in the SMB system, the packing was compressed and carbon dioxide was pumped through the packing. The pressure was increased until the needed compression was reached.

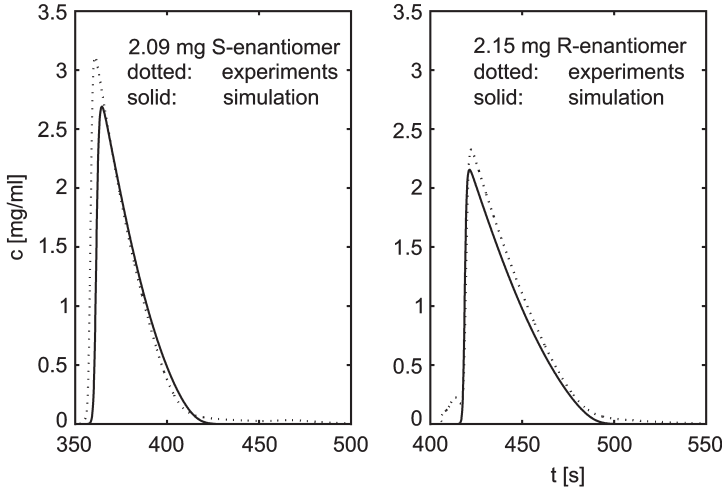

Figure 7. Experiments and simulations of single component peaks at 15.6 MPa.

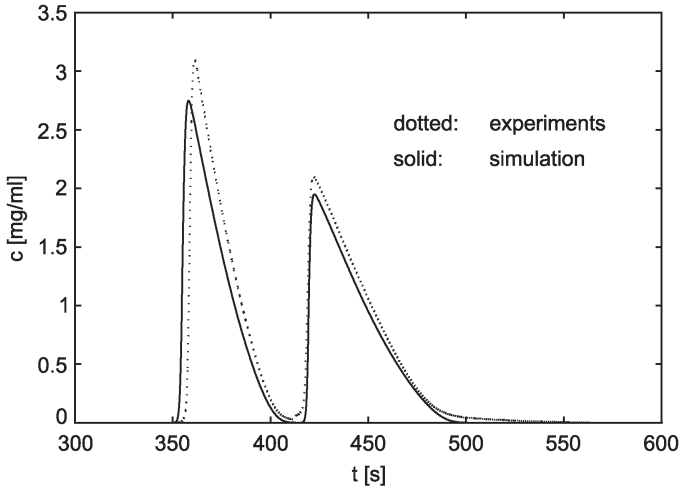

Figure 8. Experiment and simulation of mixture chromatogram (4 mg racemate at 15.6 MPa).

Each of the eight columns were tested individually in elution mode by pulse injections of *n*-hexane. The porosity of all columns packed with Kromasil are compared in Table 2; the standard variation is low (0.97%).

Separations at Low Concentration

The first set of experiments has been performed at a low concentration level to prove the feasibility of the SFC-SMB high-purity separation of the binary mixture. In the case of low concentration levels, the operating parameters can be calculated with the help of the described triangle theory. Therefore, only the porosity of the columns and the linear adsorption parameters has to be determined in subject to the density. For all experiments and simulations, mobile phase densities are calculated using the equation of state for carbon dioxide by Span and Wagner (25). As there are no density data available for the mixture used, the difference between pure carbon dioxide and mixture density is neglected.

As the pressure drop of the apparatus is known, an appropriate inlet pressure was chosen to have supercritical conditions in all zones. As described, no backpressure regulators were used for different pressure levels in the four zones of the unit. The pressure gradient in the system is generated by the pressure drop. Changing the flow rates lead to different pressure and density profiles, respectively; that leads to different linear adsorption parameters in the four zones

Table 2. Column Lengths and Porosity of the SMB Columns

	Column Number									
	1	2	3	4	5	6	7	8	Mean	SD (%)
Length (cm)	9.9	9.5	9.7	9.8	9.7	9.7	9.8	9.8	9.7	
ε	0.69	0.70	0.69	0.67	0.68	0.68	0.67	0.68	0.68	0.97

Operating Conditions: $T = 40°C$, $p = 14.5\,MPa$, IPA in $CO_2 = 4.5\,wt.\%$; injection of $100\,\mu L$ *n*-hexane; $\lambda = 220\,nm$.

of the unit. For comparison of operating points in one (m_2, m_3) plane, the pressure gradient of all runs has to be the same. For that reason, the flow rates of the different SMB runs have been kept constant, whereas the switching time has been changed. By changing the switching time at constant flow rate, we explore different separation regimes within one set of experiments without changing the level of pressure in the four zones of the unit.

The linear adsorption parameters were determined at four different pressures (14.3, 15.6, 17.9, and 20.8 MPa) by injecting a small amount of the binary mixture (0.002 mg) on an analytical column. They were calculated from the retention times of the maxima of the highly diluted chromatographic pulses. As shown in Table 3, the linear adsorption coefficients decrease with an increase in the density. This is consistent with the assumption that increasing the density leads to higher solvation power and larger elution strength of the mobile phase, respectively. Furthermore, the linear adsorption parameters at 15.6 MPa as shown in Table 3 are in good agreement with the initial slope of the nonlinear isotherms at 15.6 MPa, calculated on basis of the parameters shown in Table 1 (calculated values: 8.15 for the $S(+)$ enantiomer and 10.06 for the $R(-)$ enantiomer).

The linear adsorption parameters, according to the actual pressure in the experiments, were calculated by linear interpolation on the basis of the experimentally determined adsorption parameters.

Before starting the experiments, the exact density profile was unknown. For the calculation of the operating points, the average density for every zone was calculated on the basis of pressure at the beginning of zone 1, the temperature, and the calculated pressure drop. Subsequent to the experiments, the actual operating points were calculated on the basis of actual pressure gradient. For the determination of the boundaries of the region of complete separation in the (m_2, m_3) plane, the linear adsorption parameters of zone 2 and 3 were calculated according to the actual density of zone 2 and zone 3, respectively. The operating points in the (m_2, m_3) plane are shown in Fig. 9 together with the linear complete separation region. Purity of the extract and the raffinate predicted by the model and the obtained experimental results are in sufficient agreement (Table 4).

Table 3. Linear Adsorption Parameters

Pressure (MPa)	14.3	15.6	17.9	19.6
Density (kg/m^3)	769	789	818	837
Linear adsorption parameter $R(-)$ isomer $(-)$	10.06	8.86	7.83	7.80
Linear adsorption parameter $S(+)$ isomer $(-)$	8.21	7.26	6.37	6.10

Operating Conditions: $\dot{m}_{\text{mob. phase}} = 3.7\,\text{g/min}$, $T = 40°\text{C}$, injection volume $V_{\text{inj}} = 5\,\mu\text{L}$, IPA in $CO_2 = 4.5\,\text{wt.\%}$, $\lambda = 220\,\text{nm}$.

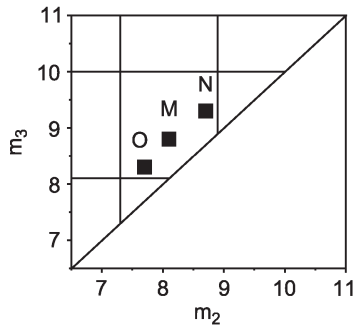

Figure 9. Operating points of the experimental racemate separations in the (m_2, m_3) plane (linear range). $T = 40°C$, 4.5 wt.% IPA in CO_2; pressure gradient 16.2/15.5/14.7/14.3 MPa.

Increasing of Feed Concentration

In the second step, the productivity of the process should be increased. The feed concentration of the components to be separated is a key factor in determining the efficiency of the separation, as well as its robustness. Increasing feed concentration causes higher productivity but lower robustness; hence the best choice of feed concentration represents a compromise between these two opposite needs.

Before analyzing the effect of operating variables on the process performance, the model for the dynamic simulation of the SFC-SMB process has to be verified. A comparison between simulation and low concentration experiments shows a good agreement (Fig. 10).

The starting point for productivity increase was SMB run M (Fig. 10) with pure raffinate and pure extract. The feed flow rate is made up of two streams: the CO_2/isopropanol flow rate and the flow rate of ibuprofen, which is dissolved in isopropanol. An increase in the feed concentration is achieved by an increase in the ibuprofen/isopropanol flow rate, whereas the total feed flow rate is held constant. As shown in Fig. 11, increasing the injected value of racemate from 20 to 60 mg/min leads to contaminated raffinate, if the operating parameters (flow rate and switching time of the valves) are not changed.

As mentioned earlier, the shape and location of the complete separation region will be changed, if the separation is characterized by nonlinear adsorption equilibrium. To show the influence of the injected amount of racemate per minute on the separation of the two ibuprofen isomers, the region of complete separation (purity $>99\%$) was calculated for different amounts of injection.

Table 4. Comparison of Model Predictions with Experimental Results of the SMB Separations

	Model Predictions		Experimental Results	
Run	Extract	Raffinate	Extract	Raffinate
O	$R(-)$, $S(+)$	Pure solvent/$S(+)$	$R(-)$, $S(+)$	>98 area-% $S(+)$
M	Pure $R(-)$	Pure $S(+)$	>99 area-% $R(-)$	>99 area-% $S(+)$
N	Pure $R(-)$	Pure $S(+)$	>98 area-% $R(-)$	$R(-)$, $S(+)$

For the calculations, a constant operating temperature ($T = 40$°C), column length ($L = 96$ mm, ID $= 30$ mm), and column configuration (two columns per zone) were assumed. Furthermore, for all calculations, the given pressure at the beginning of zone I was the same. As shown in Fig. 12, increasing the amount of injected racemate to 60 mg/min leads to a much smaller region of complete separation compared to the calculations with an injected amount of racemate of 20 mg/min. As described earlier, the separation performance is improved in terms of productivity and solvent consumption—the larger the distance of the operating point from the diagonal. On the other hand, the closer the operating point to the boundary of the region of complete separation, the higher the risk that the operating point would drive out of the complete separation region. Even small disturbances in operating conditions (flow rate or feed composition) or the effect of nonidealities (mass transfer resistance and axial dispersion) or model uncertainties (in estimation

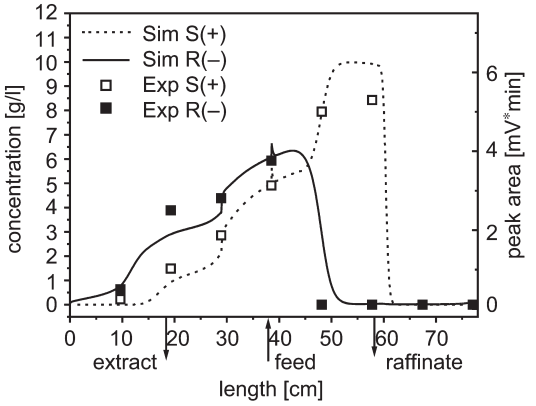

Figure 10. Internal concentration profile SMB run M (simulation and experiment) just after switching the valves (20 mg racemate/min).

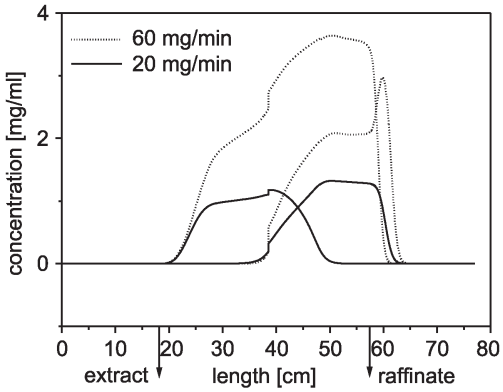

Figure 11. Simulation of SMB runs. Effect of increasing the amount of injected racemate from 20 to 60 mg/min.

of adsorption isotherm parameters) would drive the operating point out of the complete separation region. It could be seen that by increasing the feed, the position of the vertex shifts downwards to the left and the complete separation region becomes smaller and smaller, i.e., less and less robust. If the amount of injected

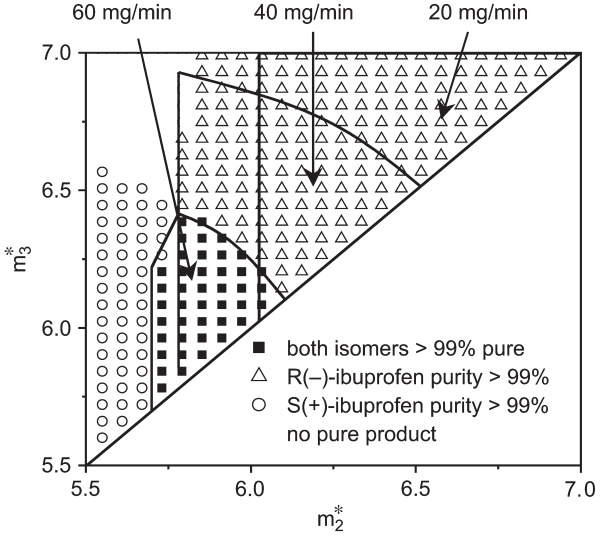

Figure 12. Region of complete separation in the (m_2^*, m_3^*) plane for injection 60 mg/min ibuprofen compared to 20 and 40 mg/min. Column configuration: 2/2/2/2.

racemate is increased to 100 mg/min, a complete separation will be impossible, which means that the maximum of productivity under the prementioned conditions is lesser than 360 $g_{racemate}/(day,kg_{stationary\ phase})$.

Changing of the Column Configuration

As mentioned previously, a complete separation is impossible if the amount of injected racemate is increased over 100 mg/min under the prementioned conditions (given pressure, temperature, and column configuration). In Fig. 13, the concentration profile is shown for an injected amount of racemate of 140 mg/min. The dotted line shows the concentration profile of the 2/2/2/2 column configuration (two columns per zone). The raffinate is contaminated by the more-retained component *R*(+)-ibuprofen. If the separation zone "zone III" is extended by one column to the 2/2/3/1 configuration, a complete separation of racemate is possible (Fig. 13, solid line). A comparison between simulation and experimental results are in good agreement. In Fig. 14, the calculated region of complete separation for injection of 140 mg/min is shown. If the amount of injected racemate is increased to 180 mg/min, a complete separation will be impossible.

In Table 5, the performance parameters for the 2/2/2/2 and the 2/2/3/1 configuration are shown. The productivity could be experimentally increased from 72 to 504 $g_{racemate}/day,kg_{stat.\ phase}$ while the consumption of CO_2 and IPA referring to the injected racemate could be reduced.

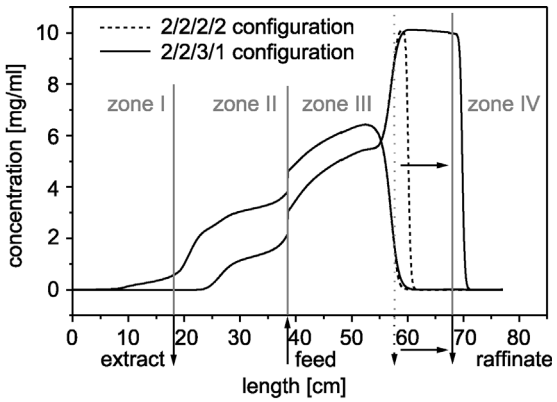

Figure 13. Concentration profile for an injected amount of racemate of 140 mg/min. Dotted line: concentration profile of 2/2/2/2 column configuration; solid line: concentration profile 2/2/3/1 column configuration.

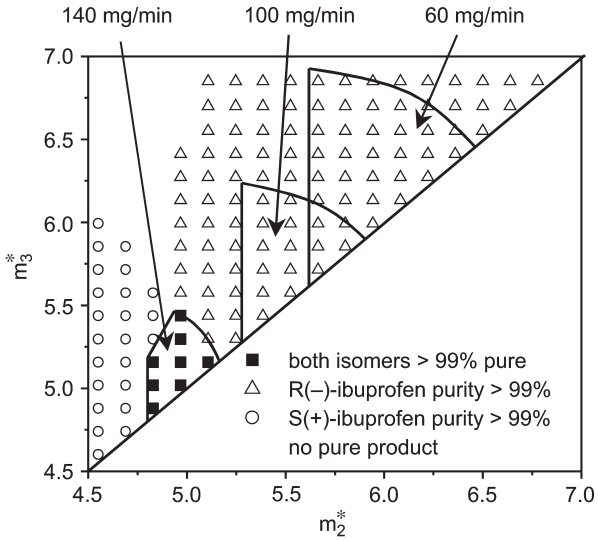

Figure 14. Region of complete separation in the (m_2^*, m_3^*) plane for injection of 140 mg/min ibuprofen compared to 60 and 100 mg/min. Column configuration: 2/2/3/1.

CONCLUSION

The SFC-SMB separation of the enantiomers was started in the linear mode with a diluted feed. A good agreement between model predictions and experimental results could be shown. The experimental SFC-SMB runs could be

Table 5. SMB Performance Parameter for the 2/2/2/2 and the 2/2/3/1 Configuration

Performance Parameter	2/2/2/2 Configuration, Experiment	2/2/3/1 Configuration, Optimized	2/2/3/1 Configuration, Experiment
Injection of racemate ($mg_{racemate}$/min)	20	140	140
Purity extract (area-%)	>99	>99	>95
Purity raffinate (area-%)	>99	>99	>99
Consumption CO_2 ($g_{CO_2}/g_{racemate}$)	590	267	280
Consumption IPA ($g_{IPA}/g_{racemate}$)	27	12	13
Productivity ($g_{racemate}$/day,$kg_{stat.\ phase}$)	72	504	504

Operating conditions: $T = 40°C$; pressure at the beginning of zone I: 17.1 MPa; $L =$ 96 mm; content of modifier: 4.5 wt.% IPA in CO_2.

described with the dynamic SMB model in combination with the measured cubic adsorption isotherm. The productivity was increased to 504 $g_{racemate}$/day,$kg_{stat.\ phase}$, while the consumption of CO_2 and isopropanol referring to the injected racemate could be reduced. However, up to now the system is not completely optimized. Only two different column configurations were investigated while column length, operating pressure, operating temperature, and content of modifier were kept constant. For example, a change of modifier might positively influence both the adsorption equilibrium and the solubility of the racemate in the mobile phase in terms of the productivity. For further optimization of the process, the influence of all parameters have to be investigated.

NOMENCLATURE

c	mobile phase concentration, kg/m^3
b,q_s,n	isotherm parameters
D	detector output, mAU
K	linear adsorption coefficient
m_j	net flow ratio
q	stationary phase loading, kg/m^3
t	time, sec
t_{inj}	injection time, sec
t_M	hold up time, sec
t_R	retention time, sec
t_{shift}	time period between two successive switches of inlet and outlet ports, sec
V	volume of the column, m^3
$\dot{V}$	volumetric flow rate, m^3/sec
V_{inj}	injection volume, m^3
V_R	retention volume, m^3
ε	overall porosity
λ	wavelength for detection, nm
ρ	density, kg/m^3

ACKNOWLEDGMENTS

The authors thank Eka Chemical for providing the stationary phase and Omya Peralta for the gifts of ibuprofen.

REFERENCES

1. Ruthven, D.M.; Ching, C.B. *Preparative and Production Scale Chromatography*; Marcel Dekker: New York, 1993; 629.
2. Ruthven, D.M. *Principles of Adsorption and Adsorption Processes*; John Wiley and Sons: New York, 1984.
3. Broughton, D.B. US Patent 3 291 726, 1966.
4. Nicoud, R.M. The Simulated Moving Bed: A Powerful Chromatographic Process. LC GC Int. **1992**, *5*, 43–47.
5. Deckert, P.; Arlt, W. Pilotanlage zur simulierten Gegenstromchromatographie—Ergebnisse für die Trennung von Fructose und Glucose. Chem. Eng. Technol. **1997**, *69*, 115–119.
6. Nagamatsu, S.; Murazumi, K.; Makino, S. Chiral Separation of a Pharmaceutical Intermediate by a Simulated Moving Bed Process. J. Chromatogr. A **1999**, *832*, 55–65.
7. Küsters, E.; Gerber, G.; Antia, F.D. Enantioseparation of a Chiral Epoxide by Simulated Moving Bed Chromatography Using Chiralcel-OD. Chromatographia **1995**, *40* (7–8), 387–393.
8. Pais, L.S.; Loureiro, J.M.; Rodrigues, A.E. Modelling, Simulation and Operation of a Simulated Moving Bed for Continuous Chromatographic Separation of 1,1-Bi-2-Naphtol Enantiomers. J. Chromatogr. A **1997**, *769*, 25–35.
9. Negawa, M.; Shoji, F.J. Optical Resolution by Simulated Moving-Bed Adsorption Technology. J. Chromatogr. A **1992**, *590*, 113–117.
10. Blehaut, J.; Charton, F.; Nicoud, R.-M. Separation of Fatty Alcohol Stereoisomers on a Large Scale High-Performance Simulated Moving Bed. LC GC Int. **1996**, *9*, 228–238.
11. Gottschlich, N.; Weidgen, S.; Kasche, V. Continuous Biospecific Affinity Purification of Enzymes by Simulated Moving-Bed Chromatography. Theoretical Description and Experimental Results. J. Chromatogr. A **1996**, *719*, 267–274.
12. Gottschlich, N.; Kasche, V. Purification of Monoclonal Antibodies by Simulated Moving-Bed Chromatography. J. Chromatogr. A **1997**, *765*, 201–206.
13. Denet, F.; Hauck, W.; Nicoud, R.-M. Continuos Supercritical Fluid Chromatographic Separation of Enantiomers in a Simulated Moving Bed Unit. Fifth International Symposium on Supercritical Fluids, Atlanta, USA, April 8–12, 2000.
14. Clavier, J.Y. A New Fractionation Process: The Supercritical Fluid Simulated Moving Bed. Seventh International Symposium on Supercritical Fluid Chromatography and Extraction, Indianapolis, March 31–April 4, 1996.

15. Depta, A.; Giese, T.; Johannsen, M.; Brunner, G. Separation of Stereoisomers in a Simulated Moving Bed-Supercritical Fluid Chromatography Plant. J. Chromatogr. A **1999**, *865*, 175–186.
16. Mazzotti, M.; Storti, G.; Morbidelli, M. Supercritical Fluid Simulated Moving Bed Chromatography. J. Chromatogr. A **1997**, *786*, 309–320.
17. Johannsen, M. Separation of Enantiomers of Ibuprofen on Chiral Stationary Phases by Packed Column Supercritical Fluid Chromatography. J. Chromatogr. A **2001**, *937* (1–2), 135–138.
18. Storti, G.; Mazzotti, M.; Morbidelli, M.; Carra, S. Robust Design of Binary Countercurrent Adsorption Separation Processes. AIChe J. **1993**, *39*, 471–492.
19. Mazzotti, M.; Storti, G.; Morbidelli, M. Optimal Operation of Simulated Moving Bed Units for Nonlinear Chromatographic Separations. J. Chromatogr. A **1997**, *769*, 3–24.
20. Gentilini, A.; Migliorini, C.; Mazzotti, M.; Morbidelli, M. Optimal Operation of Simulated Moving-Bed Units for Nonlinear Chromatographic Separations II. Bi-Langmuir Isotherm. J. Chromatogr. A **1998**, *805*, 37–44.
21. Mazzotti, M.; Storti, G.; Morbidelli, M. Supercritical Fluid Simulated Moving Bed Chromatography. J. Chromatogr. A **1997**, *786*, 309–320.
22. Migliorini, C.; Mazzotti, M.; Morbidelli, M. Continous Chromatographic Separation Through Simulated Moving Beds Under Linear and Nonlinear Conditions. J. Chromatogr. A **1998**, *827*, 161–173.
23. Rouchon, P.; Schnauer, M.; Valentin, P.; Guiochon, G. Numerical Simulation of Band Propagation in Nonlinear Chromatography. Sep. Sci. Technol. **1987**, *22*, 1793–1833.
24. Kniep, H.; Falk, T.; Seidel-Morgenstern, A. A Rapid Numerical Algorithm for Dynamic Modeling of Separation and Reaction in Simulated Countercurrent Processes. PREP, Basle, September 1–4, 1996.
25. Span, R.; Wagner, W. A New Equation of State for Carbon Dioxide Covering the Fluid Region from the Triple-Point Temperature to 1100K at Pressures up to 800 MPa. J. Phys. Chem. Ref. Data **1996**, *25*, 1509–1596.
26. Hill, T.L. *An Introduction to Statistical Thermodynamics*; Dover Publications: New York, 1986.
27. Seidel, A.; Gelbin, D. On Applying the Ideal Adsorbed Solution Theory to Multicomponent Adsorption Equilibria of Dissolved Organic Components on Activated Carbon. Chem. Eng. Sci. **1988**, *43*, 79–89.

Received April 2001
Revised January 2002